Wear 268 (2010) 1275–1284

Contents lists available at ScienceDirect

Wear

journal homepage: www.elsevier.com/locate/wear

Sliding distance, contact pressure and wear in sheet metal stamping

Michael P. Pereira [a,*], Wenyi Yan [b], Bernard F. Rolfe [c]

[a] Centre for Material & Fibre Innovation, Deakin University, Geelong, VIC 3217, Australia
[b] Department of Mechanical & Aerospace Engineering, Monash University, Clayton, VIC 3800, Australia
[c] School of Engineering, Deakin University, Geelong, VIC 3217, Australia

ARTICLE INFO

Article history:
Received 14 July 2009
Received in revised form 7 January 2010
Accepted 13 January 2010
Available online 22 January 2010

Keywords:
Sliding distance
Contact pressure
Wear
Finite element analysis
Sheet metal stamping

ABSTRACT

This paper directly examines the contact sliding distance experienced during a typical sheet metal stamping process—an area that has largely been neglected in the literature. A method to numerically quantify the sliding distance is proposed. The sliding distance predicted from this method, and the contact pressure obtained from numerical simulation, allow the recently identified time-dependent contact conditions on the die and blank surfaces to be completely characterized. Consequently, a new insight into the wear/galling that occurs at the die radius in sheet metal stamping is gained. The results show that the region close to zero degrees on the die radius is likely to experience the most wear, with the identified transient stage contributing to a large proportion of the total wear. Additionally, the region on the blank surface often observed to be heavily burnished – the die impact line – is estimated to experience the highest wear severity due to the transient contact conditions. The proposed method to numerically quantify the sliding contact conditions can be applied as a general approach to study any other two-body sliding contact situations.

1. Introduction

Tool wear has become an increasing problem in the automotive sheet metal forming industry, as a result of the implementation of higher strength steels to meet crash requirements and the reduced use of lubricants for environmental reasons. Due to the economic significance of the tool wear problem, there have been numerous studies in recent years that have aimed to experimentally characterize the wear performance of tool materials and surface treatments using representative wear tests, such as slider-on-sheet [1,2], bending-under-tension [3,4], cylindrical cup-drawing [5,6] and channel forming tests [7,8]. However, despite the large amount of research conducted and experimental data produced, reliable tool wear prediction in sheet metal stamping for particular sheet/tool material combinations and different part geometries remains a challenge. This can partly be attributed to the fact that the contact conditions that occur during sheet metal stamping are not well known. Therefore, a precise relationship between any of the 'representative' tests and the real sheet metal stamping operation cannot be made. As a result, the effectiveness of experimental testing and/or wear modeling is diminished.

There are numerous empirical-based relationships in the literature, which describe both abrasive and adhesive surface wear in sliding contact as a function of the contact conditions experienced. These include some of the well-known equations presented by Rhee [9], Bayer [10] and Archard [11], in which wear rate W is commonly expressed as a function of normal load L, sliding distance S (or sliding velocity and time), and wear coefficient K, in the following form:

$$W = KL^m S^n, \tag{1}$$

where m and n are empirical constants, fitted using data from simulative laboratory testing [12]. Therefore, for the particular system being analyzed, the accurate determination of the contact conditions – in particular contact pressure and sliding distance – is an essential step towards the estimation of wear rates and/or tool life.

There have been numerous studies that have examined, experimentally or numerically, the contact conditions that occur during continuous bending-under-tension-type processes [13–18]. Due to the steady contact conditions over the tooling radii in such operations, the sliding distance is constant and can be treated merely as a proportionality factor that can be ignored for the purposes of predicting wear rates or wear distributions. As a result, the wear response can be directly related to the contact pressure, as shown by Hortig and Schmoeckel [17].

However, it has been shown that discontinuous contact conditions exist during typical sheet metal stamping operations, such

* Corresponding author. Tel.: +61 3 5227 3353; fax: +61 3 5227 1103.
E-mail addresses: michael.pereira@deakin.edu.au (M.P. Pereira), wenyi.yan@eng.monash.edu.au (W. Yan), bernard.rolfe@deakin.edu.au (B.F. Rolfe).

0043-1648/$ – see front matter
doi:10.1016/j.wear.2010.01.020

as cup-drawing [19,20] and channel forming processes [21,22]. Although a large portion of the stamping process exhibits steady contact conditions that qualitatively compare well with bending-under-tension processes [20–22], there is an initial transient stage that exhibits severe and time-dependent contact conditions with peak contact pressures well in excess of those experienced during the steady stage [22]. As a result of the time-dependent contact conditions, the relative sliding distance between the blank and die cannot be assumed to be evenly distributed over the die radius. Therefore, the wear response is not only determined by the evaluation of contact pressure, but also by the evaluation of the sliding distance. Hence, an important step towards predicting tool wear in sheet metal stamping is to understand and characterize the amount and distribution of sliding that occurs between the blank and die throughout the forming process.

The time-dependent nature of the process will also result in discontinuous contact conditions at the blank surface, which do not necessarily mirror the conditions experienced over the die surface. As a result, a disproportionate amount of relative sliding may be experienced at particular locations on the blank surface. Considering the mechanisms of adhesive wear (galling), in which the blank material is transferred to the die, the sliding contact conditions experienced at the blank surface (as opposed to those at the die surface) may also be of primary significance. To the authors' knowledge, there have not been any studies in the literature that have directly examined the sliding distance experienced at the die radius surface, and/or at the blank surface, during sheet metal stamping processes.

This investigation utilizes finite element analysis to determine the distribution of sliding distance over the die radius during a typical channel forming operation. A method to calculate the sliding distance, and quantify the magnitude of contact pressure that occurs during the sliding contact, is proposed. It is shown that the method provides an important step towards predicting tool wear in sheet metal stamping and can be employed for other similar processes in which the varying sliding distance and contact pressure conditions have not been previously considered.

Utilizing the proposed method, the transient and steady-state contact phases experienced at the die radius, previously identified by Pereira et al. [22], are examined individually. The results show that, during the steady stage, large sliding distances are evenly distributed over the contact zone and correspond to low to moderate contact pressures. Conversely, the transient stage results in small sliding distances (up to 3 mm), at high contact pressures that are well in excess of the steady stage peak pressure. Additionally, the analysis of the conditions experienced at the blank surface shows that there is a region on the blank surface that experiences longer sliding distances at very high contact pressures. Through an estimation of the wear severity, it is shown that this region may be critical to the overall wear response.

2. Experimental and numerical setup

The channel forming process examined is shown in Fig. 1 and the main process variables are summarized in Table 1. The blank material is a Dual Phase 600 grade sheet steel (DP600), with a strain hardening index of 0.15 and yield and tensile strengths of 400 and 660 MPa, respectively. The process conditions (geometry, forming mode, blank material and thickness) were chosen as they are representative of typical auto-body structural components, such as rails, cross-members and pillars, which are often found to be prone to wear and galling [8].

The finite element model used in this study is based on the model developed by Pereira et al. [22] in a previous investigation that examined the contact pressure over the die radius during the described channel forming process. Therefore, this section will provide only a brief summary of the finite element model, as the stated reference provides a detailed description of the numerical setup, modeling procedure and analysis of the key results obtained.

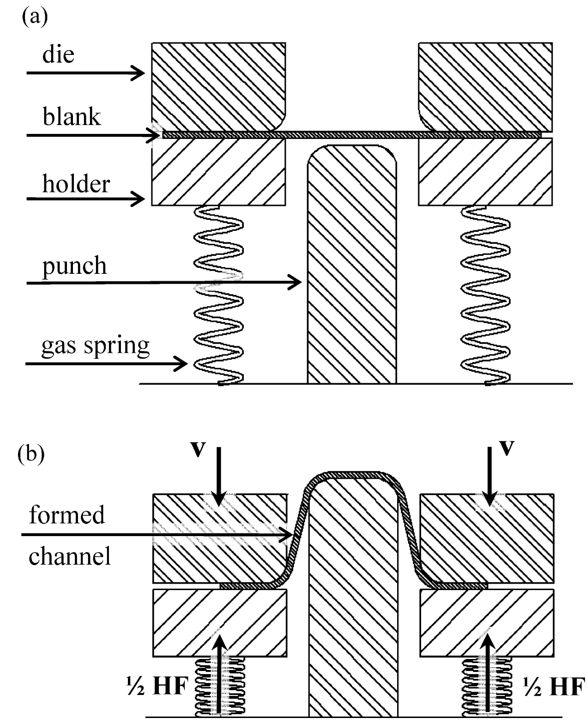

Fig. 1. Schematic of the channel forming process, (a) prior to the forming operation and (b) at the end of the forming stroke.

The channel forming process was simulated using a non-linear implicit finite element code (ABAQUS/Standard Version 6.8-1) [23]. The analysis was simplified to a one-half symmetric, two-dimensional, plane strain problem. The finite element mesh, which was significantly refined in the region of the die and blank interface, primarily consisted of four-node, bilinear, plane strain, reduced integration point, quadrilateral elements (CPE4R) with enhanced hourglass control. An elastic–plastic material definition was used for the blank, while an elastic material definition was used for the tools (die, punch and holder). An elastic modulus of 205 GPa, representing that of steel, was used for the blank and tool materials. The interactions between the blank and tool surfaces were defined using a 'hard contact' relationship for the behavior in the normal direction, and an isotropic penalty friction formulation for the tangential direction, with a friction coefficient of 0.15.

Table 1
Summary of process variables for channel forming operation.

Punch width	a	30 mm
Draw depth	d	50 mm
Final flange length	f	11 mm
Die-to-punch gap	g	2.1 mm
Blank length	l	150 mm
Initial blank holder pressure	P_h	~8 MPa
Die radius	R_d	5 mm
Punch radius	R_p	5 mm
Blank thickness	t	2 mm
Blank width	w	25 mm
Tool-to-sheet clearance (= $t - g$)	c	0.1 mm

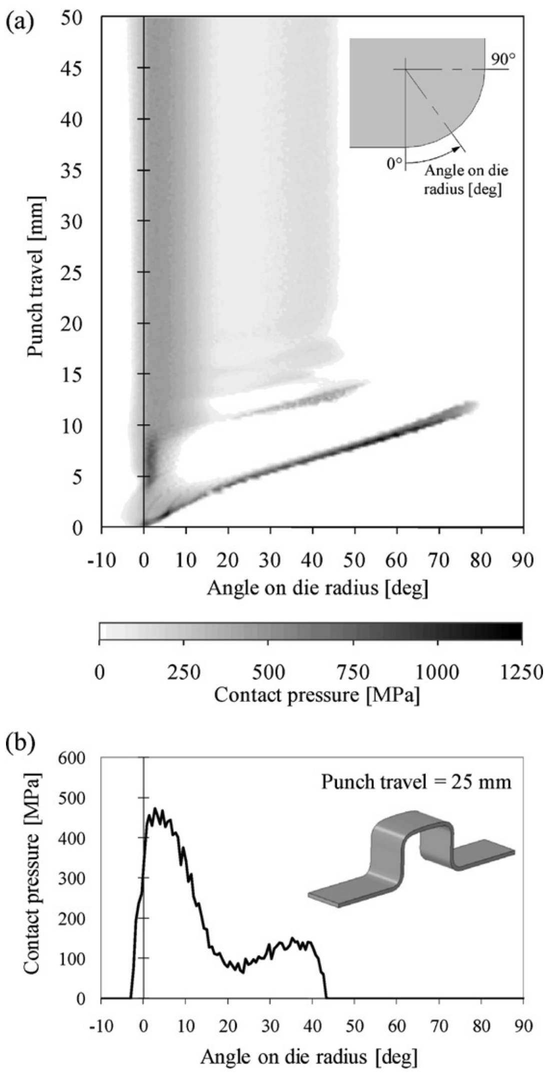

Fig. 2. (a) Contour plot showing evolution of contact pressure over the die radius throughout the duration of the forming process [22]. (b) Contact pressure distribution over die radius at a single time increment. Inset shows a 3D image of the deformed blank at that time increment (punch travel = 25 mm).

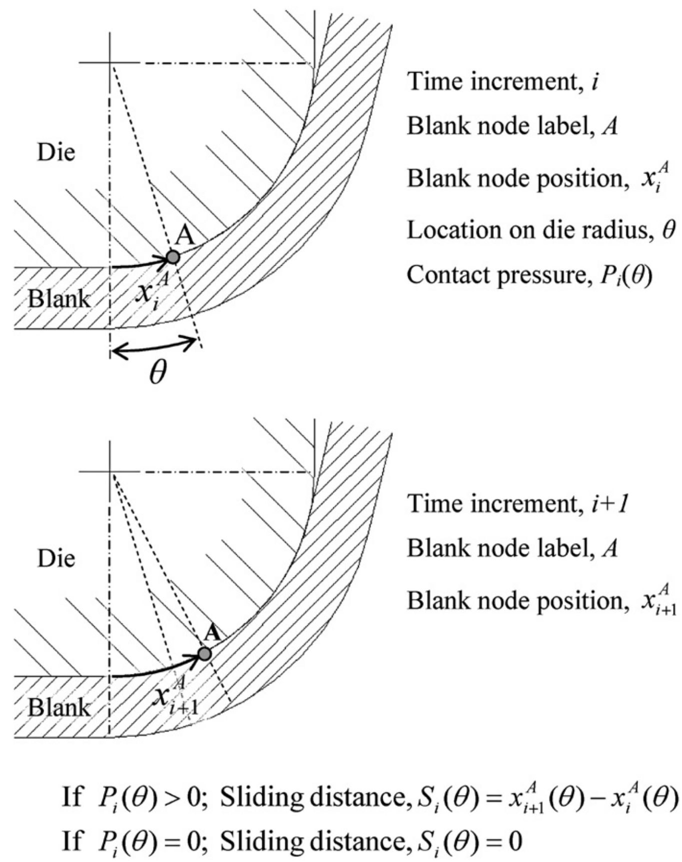

Fig. 3. Schematic showing how the incremental sliding distance between the blank and die surfaces is calculated.

3. Method for calculating sliding distance and contact pressure

3.1. Contact pressure response

Pereira et al. [22] found that the contact pressure over the die radius during the sheet metal stamping process was complex and time-dependent. However, it was shown that the entire contact pressure response could be illustrated in the form of a single contour plot, as shown in Fig. 2a. This graph was constructed by determining the contact pressure over the die radius at approximately 140 instances during the simulation results history. The abscissa represents the angular location on the die radius surface (as shown by the inset), while the ordinate represents the relative movement of the punch during the forming stroke. The contour plot can be used to determine the contact pressure over the die radius at any instant during the channel forming process, by following a horizontal line on the graph across from any value of punch travel. Then, by examining the regions where this horizontal line intersects the colored contour, the pressure distribution on the radius can be determined for that particular value of punch travel. For example, Fig. 2b shows the contact pressure distribution over the die radius obtained at the instant corresponding to 25 mm of punch travel. At this instant, it is evident that there is a large area on the die radius that does not contact the blank (zero contact pressure).

3.2. Sliding distance calculation

In order to calculate the total distance that the blank slides over the die radius, the displacement of each of the blank surface nodes during each increment of the finite element simulation must be determined. Fig. 3 shows how the incremental sliding distance, S, experienced at the location θ on the die radius, is calculated based on the movement of blank node A, from the current time increment, i, to the next time increment, $i+1$. If the contact pressure, P, occurring on the die radius at the location θ, is zero (i.e. contact does not exist between the blank and die at this location), the value calculated is merely the magnitude of displacement of the particular blank node during the current time increment. However, by only considering the instances where the contact pressure is greater than zero (i.e. when contact between the blank and die surfaces exists), the calculated displacement magnitude is equivalent to the contact sliding distance between the blank and die surfaces.

The method to calculate the contact sliding distance, $S_i(\theta)$, at the location θ on the die radius surface, during the time increment from i to $i+1$ is summarized below:

$$\begin{array}{ll} \text{If } P_i(\theta) > 0; & S_i(\theta) = x_{i+1}^A(\theta) - x_i^A(\theta) \\ \text{If } P_i(\theta) = 0; & S_i(\theta) = 0 \end{array}, \tag{2}$$

where $x_i^A(\theta)$ is the arc length position of blank node A at the location θ on the die radius surface at the time increment i, and $x_{i+1}^A(\theta)$ is the arc length position of the same material node A at the time increment $i+1$, as illustrated in Fig. 3.

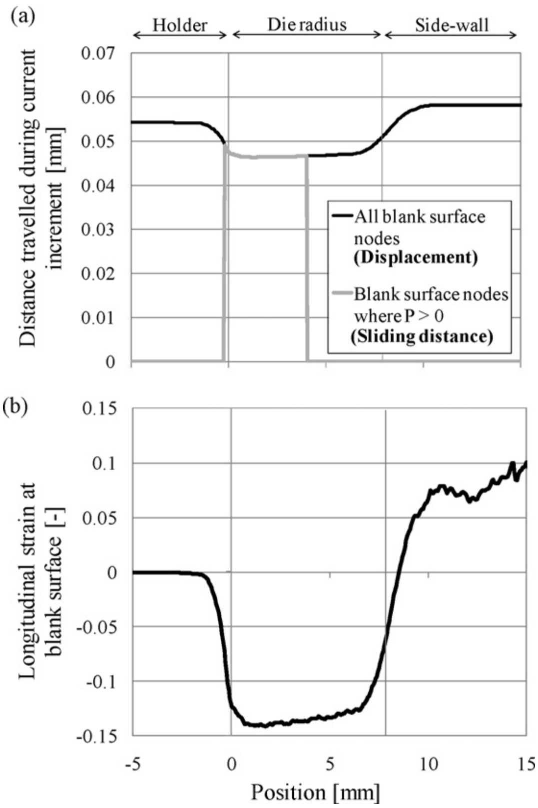

Fig. 4. (a) Sliding distance calculation for a single time increment and (b) corresponding longitudinal strain (le11) distribution at surface of blank (punch travel = 25 mm).

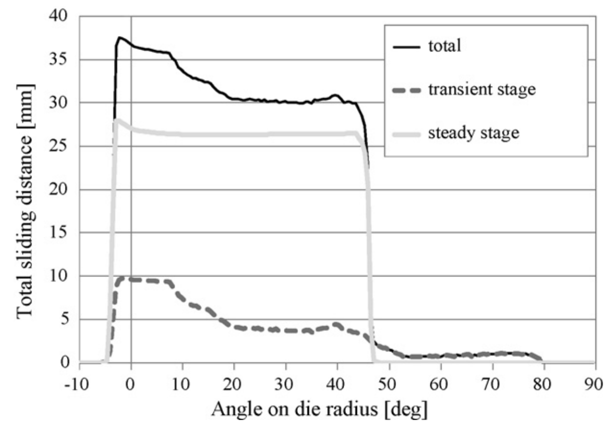

Fig. 5. Total sliding distance distribution experienced over the die radius surface during the channel forming process.

The effect of considering only the instances where contact pressure exists is shown in Fig. 4a, where the displacement magnitude and sliding distance for all blank surface nodes during a single increment was calculated. The abscissa in Fig. 4a represents the position in mm of the blank surface nodes (instead of the previously denoted angular position on the radius, due to the larger region of the blank surface examined). As shown, the die radius corresponds to the region between 0 and 7.8 mm, while the locations before and after the die radius correspond to the holder and side-wall regions, respectively.

Fig. 4a shows that the displacement varies from node to node over the blank surface, indicating that each node did not travel the same distance during the particular time increment. This uneven distribution of movement at the blank surface occurs throughout the simulation results history and is a direct result of the deformation at the surface of the blank. As shown by the longitudinal strain distribution in Fig. 4b, the blank surface experiences significant compressive strain at the die radius region (up to 14% at the increment shown). Therefore, the length of the blank, and the resulting sliding distance, is effectively reduced at the region where the blank contacts the die radius. Additionally, Fig. 4b shows that the side-wall region of the blank experiences tensile strains (up to 10% at the increment shown). This has the effect of reducing the sliding distance further, because the drawing action of the punch is reduced as the blank side-wall stretches.

Using the method described above and summarized in Eq. (2), the sliding distance distribution shown in Fig. 4a was obtained for each increment of the simulation results history, through the use of a Python script. The location on the die radius at which the sliding distance was calculated, corresponds to the location of the contacting blank nodes at each time increment. Therefore, in a similar way to obtaining the contact pressure data (described in [22]), the sliding distance distribution data at each solution increment was standardized (through interpolation) to achieve a consistent location for the angle along the die radius. The standardized interval γ was set to 0.57° (corresponding to an arc length of 0.05 mm). Therefore, the standardized locations on the die radius are $\varphi = 0$, γ, 2γ, 3γ, etc.

By accumulating the sliding distance calculated at each standardized location on the die radius, the total sliding distance distribution over the radius was determined, as shown in Fig. 5. The total sliding distance experienced at any standardized location φ on the die radius is the summation of the sliding distance at the same location for the entire simulated stamping process, i.e.:

$$S(\varphi) = \sum_{i} S_i(\varphi) \tag{3}$$

where i represents an arbitrary time increment in the numerical simulation.

For the purposes of wear analyses, the total sliding distance shown in Fig. 5 does not provide enough information into the likely wear response over the die radius, because the magnitude of contact pressure during the relative sliding is unknown. Since the contact pressure is a key factor, the sliding distance must be studied in combination with the contact pressure. To achieve this, a series of contact pressure levels (bins) were defined at 100 MPa intervals, beginning at 0 MPa up to the maximum contact pressure experienced during the process (i.e. $0 < P \leq 100$, $100 < P \leq 200$, etc.). The Python script was modified to consider the magnitude of contact pressure that occurred at each point on the die radius, in order to allow the incremental sliding distance to be accumulated into the separate bins of contact pressure. Therefore, the total sliding distance graph in Fig. 5 was essentially divided into a series of graphs, to allow the sliding distance experienced at each of the defined intervals of contact pressure to be shown (see Fig. 6).

It is evident that the single graph shown in Fig. 6a summarizes the contact conditions (both sliding distance and contact pressure) that occur throughout the entire forming process. The method presented here can be adopted to determine the time-dependent contact conditions of any other process which exhibits similar two-body contact.

4. Results and discussion

This section discusses the results obtained for the overall contact conditions at the die radius in further detail, and also separately examines the response during the previously identified transient and steady-state stages of the channel forming process. Addition-

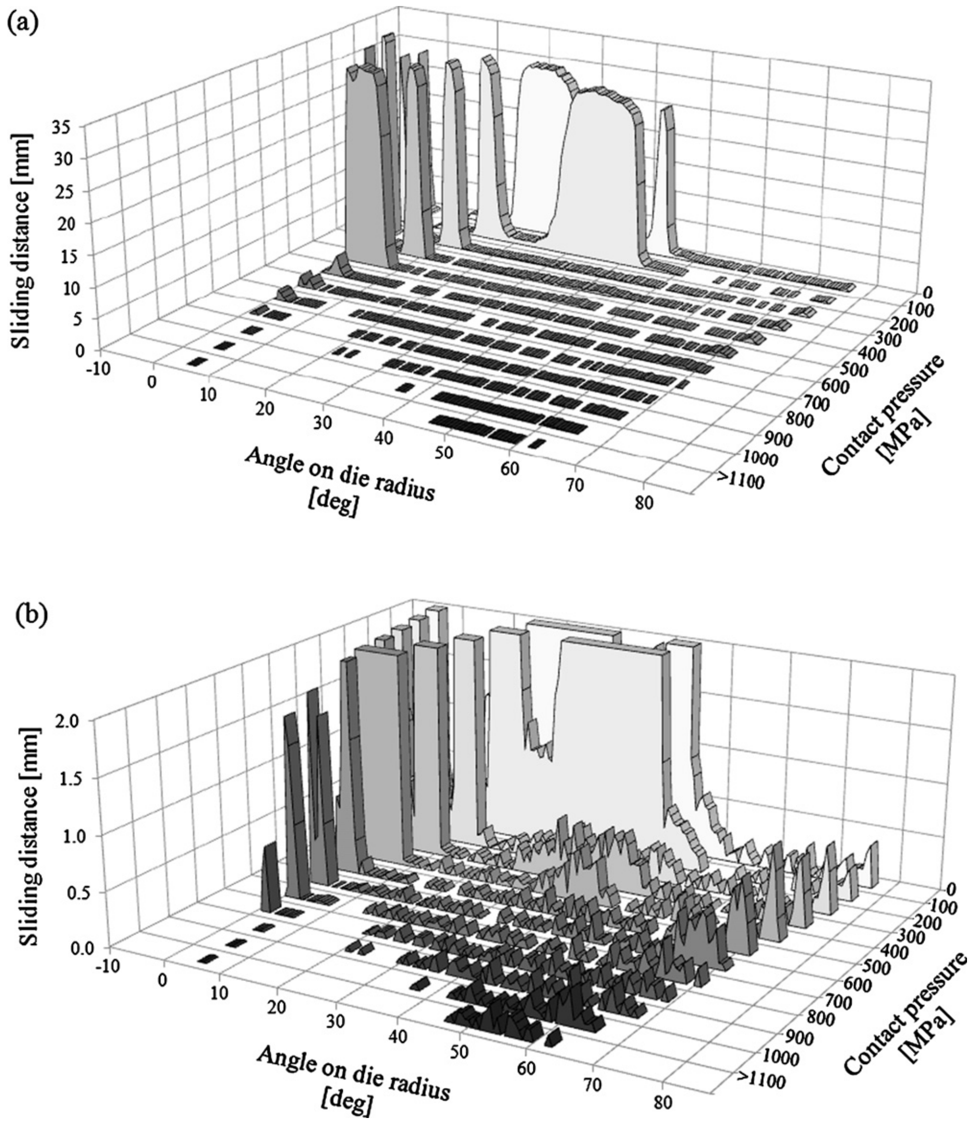

Fig. 6. Sliding distance over the die radius at each of the defined contact pressure intervals (a) for all the values of sliding distance, and (b) truncated to show sliding distance values below 2.0 mm (permitting the small sliding distances, at higher values of contact pressure, to be shown more clearly).

ally, the proposed method for determining the contact conditions is applied to consider the relative sliding distance and contact pressure experienced from the perspective of the blank surface (as opposed to those experienced by the die radius surface). Finally, the results obtained from these analyses easily lend themselves to the application of available wear models/equations to estimate wear rates. As such, the possible wear behavior over the die radius and at the blank surface is also estimated and discussed.

4.1. Overall contact conditions at the die radius

The previous analysis of the contact pressure over the die radius by Pereira et al. [22] revealed that the response consisted of two distinct phases, as can be seen in Fig. 2a. The first stage was described as a transient phase, characterized by highly localized and severe contact pressures that occurred over a large proportion of the radius. The second stage, which existed for the majority of the process, exhibited steady contact conditions that occurred over approximately the first half of the die radius. The smooth, two-peak contact pressure distribution during this stage (as shown in Fig. 2b) was similar to that expected from continuous bending-under-tension processes. The peak pressures experienced during the transient phase of the process, which were more than double the magnitude of the steady stage peak pressures, were shown in a subsequent analysis to be the result of the bending stress and line contact conditions that occur as the initially straight blank is wrapped over the curve die radius surface [21]. The overall maximum pressure, P_{max}, was found to be 1247 MPa and occurred during the transient stage of the process at 58.5° on the die radius. While the maximum contact pressure during the steady stage, P_{steady}, was determined to be 499 MPa, occurring at 5.5° on the die radius [22].

Figs. 5 and 6 further highlight the varied contact conditions experienced over the die radius during the channel forming process. Fig. 5 shows the total amount of sliding experienced over the die radius surface, where it is evident that the maximum sliding distance of 37.5 mm occurs at the region just prior to the start of the die radius (at −2.3°). The total sliding distance reduces to approximately 30 mm at the region between 20° and 40° on the die radius. Further along the radius, where contact between the blank and die surfaces only occurs during the transient portion of the process (the region between 50° and 80°), only approximately 1 mm of total sliding occurs.

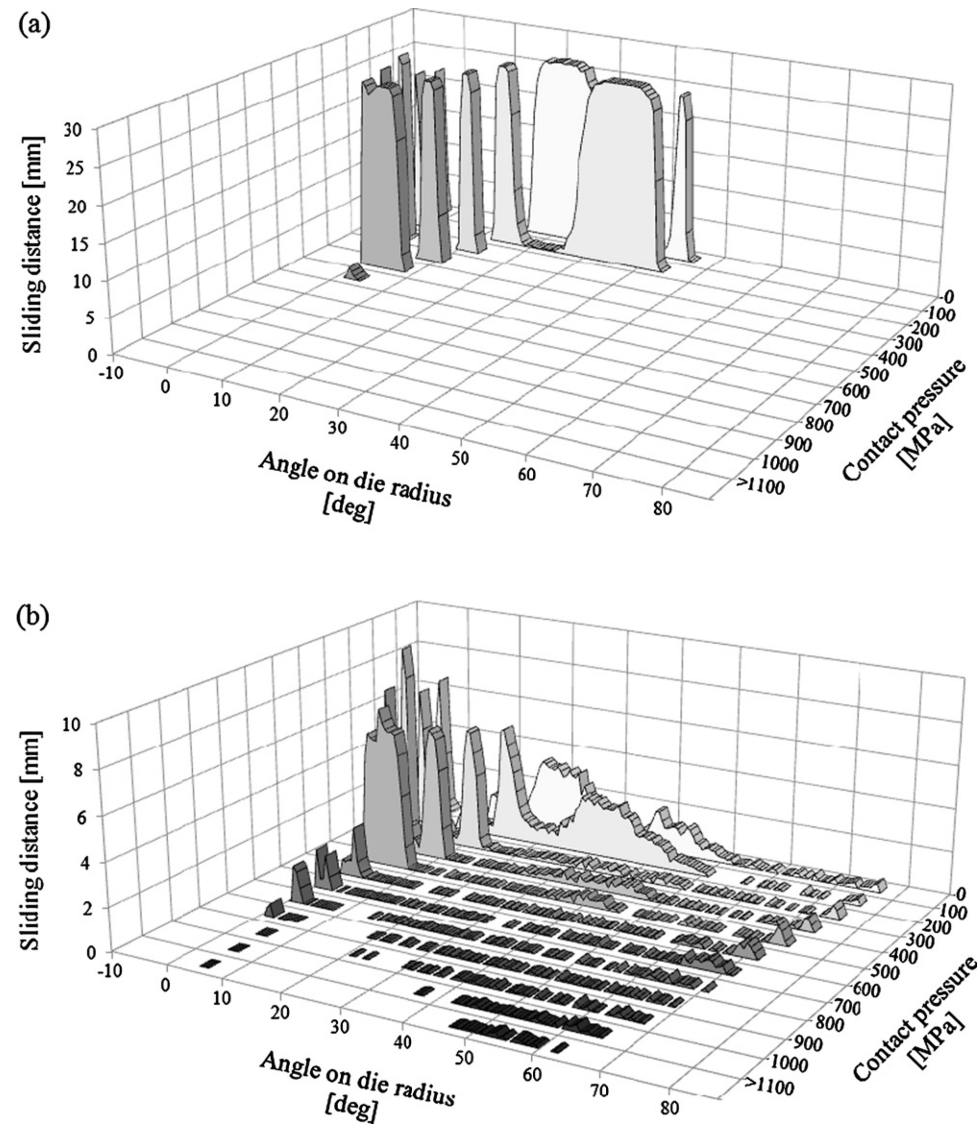

Fig. 7. Contact conditions occurring over the die radius during the two identified stages of the channel forming process: (a) steady-state stage (punch travel = 17–50 mm); (b) transient stage (punch travel = 0–17 mm).

Fig. 6 shows that the large sliding distances, which occur at angles below 50° on the die radius, correspond to low to moderate contact pressures (between 0 and 500 MPa). While the small magnitude of sliding experienced at locations greater than 50° on the die radius, mainly correspond to large contact pressures (greater than 500 MPa). It is evident that these two notably different types of contact conditions closely correspond to the identified steady and transient stages, respectively.

4.2. *Contact conditions at the die radius during steady and transient stages*

The analysis detailed in Section 3.2 was repeated in order to separately examine the contact conditions that occur during the two distinct stages of the channel forming process. Fig. 5 shows the total sliding distance accumulated during the transient and steady stages individually, while Fig. 7 summarizes the contact conditions for each of these stages.

As expected, it is evident that the steady stage results in very consistent contact conditions over the die radius. Fig. 5 shows that a sliding distance of approximately 27 mm is experienced over almost the entire contact zone (i.e. between the region of −4° to 47° on the die radius). This even sliding distribution is a result of the steady nature of this stage, which closely resembles a bending-under-tension-type process. *New* blank material continually enters the contact zone, where it is plastically bent to conform to the

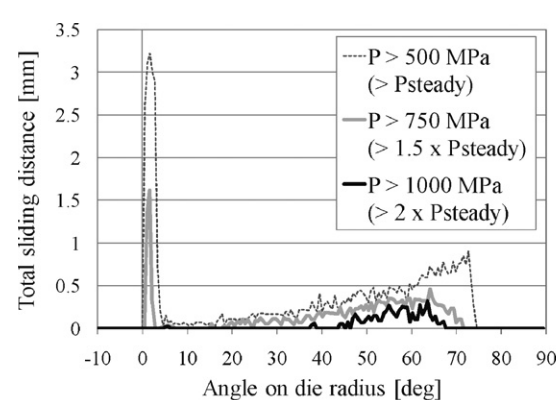

Fig. 8. Sliding distance experienced over the die radius during the transient stage at contact pressures above the steady-state peak contact pressure (P_{steady}).

radius, and remains in contact with the die until it is partially straightened and loses contact with the die [21]. Hence, it is clear that the steady-state phase is characterized by large sliding distances at low to moderate contact pressures, which occur over only the first half of the die radius.

In contrast to the steady-state phase, Figs. 5 and 7b show that the transient stage consists of markedly varied contact conditions. Approximately 9 mm of sliding occurs near the region of 0° on the die radius, at contact pressures below 500 MPa, indicating that part of the transient phase exhibits contact conditions that are similar in magnitude and location to that of the steady-state stage. However, as discussed by Pereira et al. [22], there is a region on the die radius that only makes contact with the blank during the transient stage, and not during the steady-state stage – i.e. a *transient-only* contact region. In this case, this transient-only zone corresponds to the region between 45° and 80° on the die radius.

If only the contact pressures greater than those observed during the steady-state phase (P_{steady}) are considered, it is evident these contact conditions result in a much smaller amount of sliding, as shown in Fig. 7b and more clearly in Fig. 8. Interestingly, these high contact pressure sliding events occur over the majority of the radius, albeit to a varying degree. The total sliding distance during the transient stage, for contact pressures above P_{steady}, is approximately 3.2 mm near the region of zero degrees on the die radius. While in the *transient-only* contact region, up to 0.9 mm of sliding distance occurs near 70° on the die radius, at contact pressures greater than P_{steady}. Furthermore, the sliding conditions with very high contact pressures (greater than 1000 MPa) primarily occur in this transient-only region, but result in very small sliding distances (less than 0.35 mm).

Although only a small amount of total sliding distance is experienced for contact pressures above P_{steady}, it is possible that these conditions may be important to the wear response. In a real production process, where many thousands of components are stamped using a single die tool, these high contact pressure, but small sliding distance, events will result in several tens or hundreds of meters of total sliding.

4.3. Wear estimation at the die radius

The fact that the combined contact pressure and sliding distance conditions have been quantitatively determined in this study permits the easy application of available wear models/equations. Hence, an insight into the possible wear behavior over the die radius for the channel forming process can be obtained.

The well-known general wear equation, shown in Eq. (1), can be used to describe both abrasive and adhesive surface wear behavior for sliding contacts. Therefore, by using this equation and the values of contact pressure and sliding distance predicted over the die radius (as graphed in Figs. 6 and 7), it is possible to estimate the distribution of wear over the die radius for the entire channel forming process, as shown in Fig. 9.

Although the empirical constants in Eq. (1) are usually fitted using data from simulative laboratory testing, in general, it has been observed that $m \geq 1$ (with typical values in the range of 2–3), and $n \leq 1$ [24]. Hence, the values of m and n were chosen within this range for the purposes of this illustration. The values of wear are shown in Fig. 9 without units, as the purpose of this analysis is to show the possible trends in wear over the die radius by utilizing the knowledge of the contact conditions obtained through the method proposed in this study. For this reason, the effect of the wear coefficient K can be ignored, as it is merely a constant that will not change the shape of the estimated wear distributions shown in Fig. 9.

For the range of empirical constants shown, it is evident that the wear equation predicts that the region close to the beginning of the die radius is likely to experience the most wear, and therefore

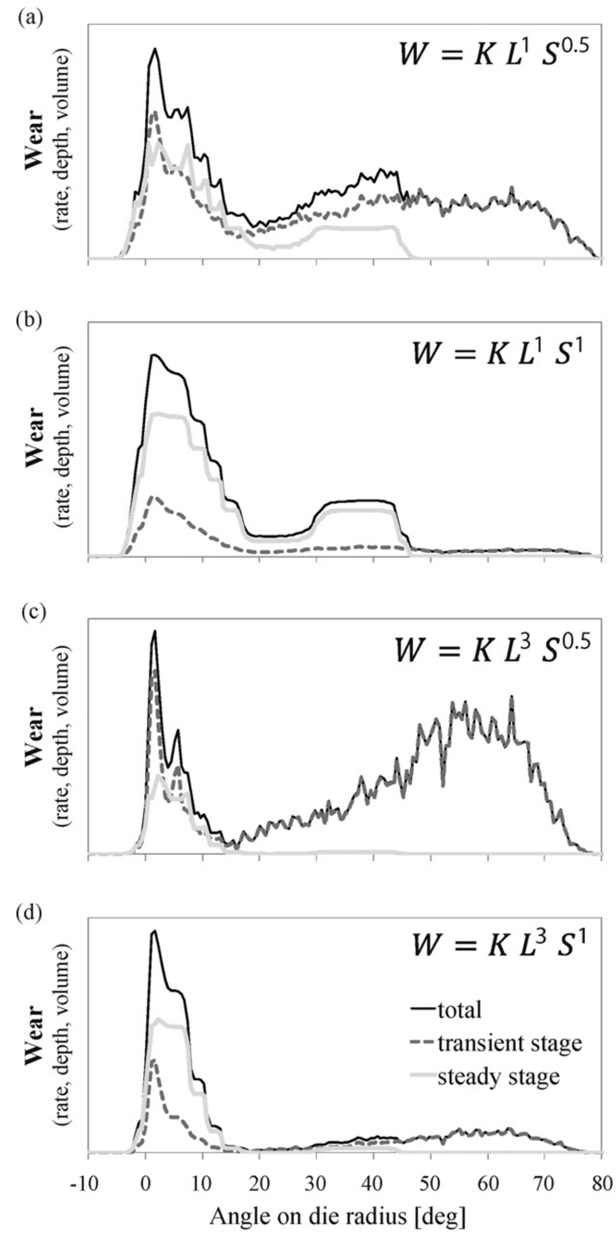

Fig. 9. Possible trends of wear over the die radius, as calculated using the general wear equation shown.

be critical to the overall wear response. This response qualitatively compares well with the experimental wear profiles and numerical predictions presented in recent studies of a cylindrical cup-drawing process [5,6].

It was previously speculated by Pereira et al. [21,22] that the transient stage of the process and the transient-only contact region may be of primary significance to the wear response. This was because: severe contact pressure conditions were found to occur during the transient stage; the maximum contact pressure exists in the transient-only contact region; and that the wear rate has been found to be very sensitive to the maximum contact pressure [25]. Therefore, the trends shown in Fig. 9 may initially appear to be contradictory to this previous notion.

However, in addition to showing the total wear distribution, Fig. 9 also shows the wear response calculated for the transient and steady-state stages of the channel forming process. In each case, the wear equation was used to calculate the wear severity based on the accumulated sliding distance and contact pressure data associated with each of the phases (i.e. the data shown graphically in Fig. 7). In our numerical calculation, the wear at any location φ on the die radius is the summation of the wear occurring during every contact pressure interval, at the same location, for the entire simulated stamping process, i.e.:

$$\begin{aligned} W_{total}(\varphi) &= \sum_j K(P_j(\varphi))^m (S_{j,\ total}(\varphi))^n \\ W_{steady}(\varphi) &= \sum_j K(P_j(\varphi))^m (S_{j,\ steady}(\varphi))^n \\ W_{transient}(\varphi) &= \sum_j K(P_j(\varphi))^m (S_{j,\ transient}(\varphi))^n \end{aligned} \quad , \qquad (4)$$

where j represents an arbitrary contact pressure interval as shown in Fig. 7, and P_j is taken as the mean pressure of the interval j. For example, $P_j = 50$ MPa for the contact pressure interval j: $0 < P \leq 100$ MPa. When the sliding distance exponent n is equal to 1, the sum of the wear contributions calculated for the transient and steady stages is equal to the total wear shown. However, when the exponent n is not equal to 1, the sum of the transient and steady wear values is not equal to the total wear – i.e. $(S_{j,total}(\varphi))^n \neq (S_{j,steady}(\varphi))^n + (S_{j,transient}(\varphi))^n$, although $S_{j,total}(\varphi) = S_{j,steady}(\varphi) + S_{j,transient}(\varphi)$. This is due to the non-linear variation of wear with sliding distance and is shown by the curves in Fig. 9a and c. In these instances, the wear distribution shown would be the response expected to occur if the conditions associated with each stage occurred individually on the die radius surface.

The trends shown in Fig. 9 indicate that, depending on the values of m and n, the contact conditions experienced in the transient stage of the process may contribute to the most amount of wear at the die surface. Unfortunately, the values of the exponents provide little insight into the type or severity of the wear that could cause such behavior, and must be determined from experimental tests [24]. Nevertheless, regardless of the value of the empirical exponents, it is evident that the transient stage is likely to contribute significantly to the total wear response at the die radius, and hence be important to the overall wear behavior, as initially speculated.

Considering the results presented in Fig. 7, it is evident that the majority of the die radius surface experiences significantly varied contact conditions. The conditions experienced by almost any single location on the die radius can range from low to moderate contact pressures with large sliding distances, to severe contact

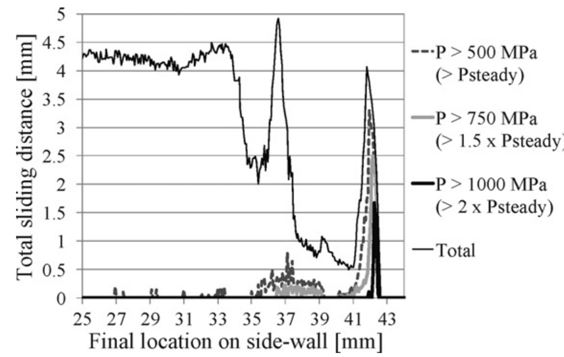

Fig. 11. Sliding distance experienced on the blank surface during the channel forming process at contact pressures above the steady-state peak contact pressure (P_{steady}).

pressures with small sliding distances. Therefore, it is possible that a severe contact pressure event may initiate wear/galling at a particular location on the die radius. This same region on the die radius surface may then experience large sliding distances and moderate contact pressures, which may not have been previously sufficient to initiate galling. However, considering the galling initiation/lump growth theories presented in the literature [26,27], it is likely that this small lump of galling may then rapidly grow during the lower contact pressure sliding events and cause eventual failure of the tooling. Hence, the overall wear response over the die radius may be a direct result of these varied contact conditions, and therefore will not be captured through the use of an empirical wear model initially derived using steady contact conditions. Similarly, traditional wear tests (such as pin-on-disc or bending-under-tension tests) are largely steady-state processes and therefore cannot replicate the discontinuous contact conditions associated with the channel forming process. Therefore, the applicability of traditional wear tests and models for the simulation of wear in sheet metal stamping may be questionable.

4.4. Contact conditions at the blank surface

Galling (adhesive wear) has traditionally been analyzed by examining the conditions experienced over the tool surface. The galling mechanism results in the transfer of softer sheet material

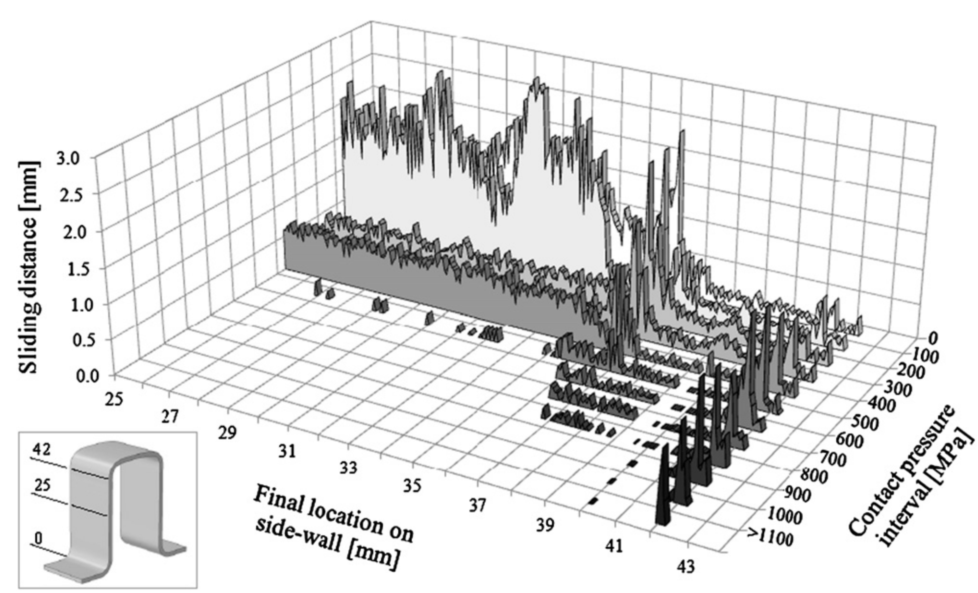

Fig. 10. Contact conditions occurring on the blank surface during the channel forming process. The inset shows the corresponding location on the deformed blank surface.

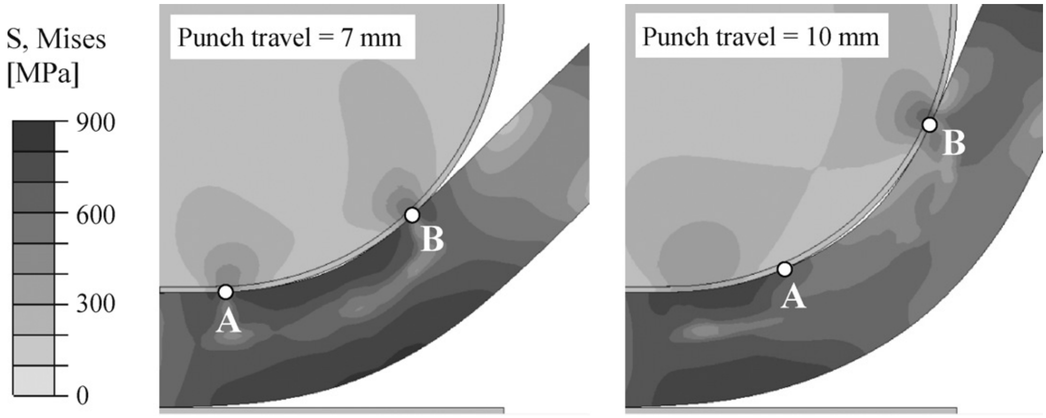

Fig. 12. Blank movement and deformation at two instances during the channel forming process, showing how a single location on the blank surface (Point B) does not pass through the contact zone.

to the hard tool surface [26,27] and, in effect, can be considered as wear of the sheet material. Therefore, it is possible that the conditions experienced by the surface of the blank, as opposed to those experienced by the tooling surface, may be of importance to the wear response. Furthermore, the traditional assumption that new blank material continually enters the contact zone may be inappropriate due to the discontinuous contact conditions shown in this study, as will be explained below.

The procedure for determining the contact conditions, presented above, can be employed for other similar processes in which the time-dependent sliding distance and contact pressure conditions have not been previously considered. Therefore, this procedure will be applied to investigate the relative sliding distance and contact pressure experienced from the perspective of the blank surface during the channel forming process. The analysis will be primarily focused on the region known as the 'die impact line', which is a clear demarcation visible on the side-wall after the forming operation. This line separates the burnished material that has travelled over the die radius and the free surface that has not contacted the tooling [28], and corresponds to the region that experiences the severe and discontinuous contact conditions during the transient stage.

The results of the analysis of the contact conditions occurring on the blank surface during the channel forming process are shown in Figs. 10 and 11. The blank surface continually moves during the forming operation. Therefore, the contact conditions experienced throughout the process are plotted with respect to the final location on the blank surface. This location is represented by the vertical height on the side-wall, as shown in the inset in Fig. 10. The region near 42 mm on the side-wall corresponds to the die impact line, as Fig. 10 shows that the blank does not make contact with the die surface above this location. Conversely, the region below approximately 33 mm on the side-wall experiences approximately constant sliding conditions and corresponds to the region of the blank that makes contact with the die radius during the steady-state stage of the forming process. Hence, the contact pressures experienced on the blank in this region are less than or equal to P_{steady}. As expected, the sliding distance of approximately 4 mm experienced in this region (as shown in Fig. 11) closely corresponds to the length of contact between the blank and die radius during the steady-state stage.

The region on the side-wall between 33 and 42.5 mm corresponds to the area of the blank that makes contact with the die during the transient stage, as evidenced by the discontinuous contact conditions shown in Fig. 10. Fig. 11 shows that the location near 42 mm on the side-wall experiences over 3 mm of sliding at contact pressures over 500 MPa, and approximately 1.7 mm of sliding at pressures over 1000 MPa.

Close examination of the contact pressure contour in Fig. 2a can reveal the contact length, at any single instant, between the blank and die radius. During the high contact pressure events of the transient stage, it is evident that the contact length does not exceed 10° on the die radius (i.e. 0.9 mm arc length). Therefore, the larger sliding distances at high contact pressures occur because the same region on the blank surface remains in contact with the die as the angle of wrap is increased, as illustrated in Fig. 12. In this figure it is evident that, as the punch draws new material over the die radius, Point A on the blank surface clearly passes through the high pressure contact zone, as expected. Therefore, Point A only experiences small sliding distances at the high contact pressures. However, the second contact zone, experienced by Point B on the blank surface, does not remain stationary during the process. Therefore, instead of new material continuously passing through the contact zone, Point B remains in contact with the die radius. As a result, Point B experiences longer sliding distances at high contact pressures. It is possible that this phenomenon may play an important role in the wear/galling response for particular sheet and tool material combinations.

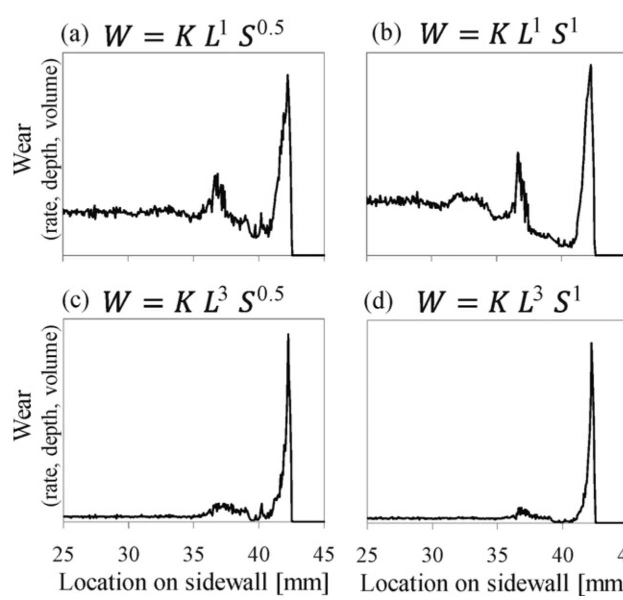

Fig. 13. Possible trends of wear on the blank surface, as calculated using the general wear equation shown.

4.5. Wear estimation at the blank surface

In order to gain an insight into the possible wear behavior, the general wear equation was applied for the contact conditions experienced at the blank surface. Fig. 13 shows that, for the range of empirical constants examined, the estimated wear on the blank surface is most severe at the die impact line, with a significant drop in wear severity immediately after this region.

If the side-wall of a typical channel-type part is examined after the forming operation, there is often a small area of blank material at the die impact line that is more severely burnished than the other regions. Careful examination of the photographs of the side-wall of stamped channel components presented by Liljengren et al. [7,29] reveals this phenomenon. This highlights that severe surface effects exist in this region and emphasizes the possible significance of these identified contact conditions to the overall tool wear response.

5. Summary

This paper directly examines the contact sliding distance experienced during a typical sheet metal stamping process—an area that has largely been neglected in the literature. A method to numerically quantify the sliding distance was proposed. The sliding distance predicted from this method, and the contact pressure obtained from numerical simulation, allowed the recently identified time-dependent contact conditions on the die and blank surfaces to be completely characterized. As a result, a new insight into the wear occurring at the die radius in sheet metal stamping was gained.

It was shown that the steady-state phase resulted in consistent contact conditions over the first half of the die radius, with moderate contact pressures and large sliding distances. Conversely, the transient phase resulted in varied contact pressures, over a large portion of the die radius. At contact pressures above those experienced during the steady-state phase, small sliding distances occurred. It was shown that the region close to zero degrees on the die radius is likely to experience the most wear, with the transient contributing to a large proportion of the total wear.

Analysis of the contact conditions experienced by the blank showed that there is a region on the blank surface that experiences longer sliding distances at very high contact pressures. Additionally, the region on the blank surface often observed to be heavily burnished – the die impact line – was estimated to experience the highest wear severity and shown to be a result of the transient contact conditions. Therefore, the analysis of the conditions at the die and blank surfaces both showed that the identified transient stage is likely to be critical to the overall wear/galling behavior.

This study further develops the understanding of the contact conditions occurring during sheet metal stamping, and will assist with future wear investigations. Additionally, the proposed method to numerically quantify the sliding distance can be applied as a general approach to study any other two-body sliding contact situations.

Acknowledgements

This research was supported by Ford Motor Company USA, Ford of Australia, Volvo Cars Sweden, and an Australian Research Council Linkage Project (LP0776913). The authors extend their gratitude to Professor Peter Hodgson from Deakin University for his support.

References

[1] A. Gåård, P. Krakhmalev, J. Bergström, N. Hallbäck, Galling resistance and wear mechanisms—cold work tool materials sliding against carbon steel sheets, Tribol. Lett. 26 (2007) 67–72.
[2] E. van der Heide, E.D. Stam, H. Giraud, G. Lovato, N. Akdut, F. Clarysse, P. Caenen, I. Heikillä, Wear of aluminium bronze in sliding contact with lubricated stainless steel sheet material, Wear 261 (2006) 68–73.
[3] M.J. Alinger, C.J. Van Tyne, Evolution of die surfaces during repeated stretch-bend sheet steel deformation, J. Mater. Process. Technol. 141 (2003) 411–419.
[4] C. Boher, D. Attaf, L. Penazzi, C. Levaillant, Wear behaviour on the radius portion of a die in deep-drawing: identification, localisation and evolution of the surface damage, Wear 259 (2005) 1097–1108.
[5] K. Ersoy-Nürnberg, G. Nürnberg, M. Golle, H. Hoffmann, Simulation of wear on sheet metal forming tools—an energy approach, Wear 265 (2008) 1801–1807.
[6] H. Hoffmann, G. Nürnberg, K. Ersoy-Nürnberg, G. Herrmann, A new approach to determine the wear coefficient for wear prediction of sheet metal forming tools, Prod. Eng. 1 (2007) 357–363.
[7] M. Liljengren, K. Kjellsson, D. Wiklund, Guidelines for die materials, hardening methods and surface coatings for forming of high, extra high and ultra high strength steel sheets (HSS/EHSS/UHSS), in: Proc. IDDRG 2008 Conference, Olofström, Sweden, 2008, pp. 603–614.
[8] O. Sandberg, P.-Å. Bustad, B. Carlsson, M. Fällström, T. Johansson, Characterisation of tool wear in stamping of EHS and UHS steel sheets, in: Proc. International Conference on Recent Advances in Manufacture & Use of Tools & Dies and Stamping of Steel Sheets, Olofström, Sweden, 2004, pp. 151–170.
[9] S.K. Rhee, Wear equation for polymers sliding against metal surfaces, Wear 16 (1970) 431–445.
[10] R.G. Bayer, A general model for sliding wear in electrical contacts, Wear 162–164 (1993) 913–918.
[11] J.F. Archard, Contact and rubbing of flat surfaces, J. Appl. Phys. 24 (1953) 981–988.
[12] S.M. Hsu, M.C. Shen, A.W. Ruff, Wear prediction for metals, Tribol. Int. 30 (1997) 377–383.
[13] D. Attaf, L. Penazzi, C. Boher, C. Levaillant, Mechanical study of a sheet metal forming dies wear, in: Proc. 6th International Tooling Conference, Karlstad, Sweden, 2002, pp. 209–221.
[14] G.J. Coubrough, M.J. Alinger, C.J. Van Tyne, Angle of contact between sheet and die during stretch-bend deformation as determined on the bending-under-tension friction test system, J. Mater. Process. Technol. 130–131 (2002) 69–75.
[15] M. Eriksen, The influence of die geometry on tool wear in deep drawing, Wear 207 (1997) 10–15.
[16] K. Hanaki, K. Kato, Pressure peak in bending and unbending process, Adv. Technol. Plastic. 1 (1984) 581–586.
[17] D. Hortig, D. Schmoeckel, Analysis of local loads on the draw die profile with regard to wear using the FEM and experimental investigations, J. Mater. Process. Technol. 115 (2001) 153–158.
[18] Y.S. Kim, M.K. Jain, D.R. Metzger, Non-uniform pressure distribution in draw-bend friction test and its influence on friction measurement, in: Proc. NUMISHEET 2005 Conference, Detroit, MI (USA), 2005, pp. 661–666.
[19] M.R. Jensen, F.F. Damborg, K.B. Nielsen, J. Danckert, Applying the finite-element method for determination of tool wear in conventional deep-drawing, J. Mater. Process. Technol. 83 (1998) 98–105.
[20] J. Mortensen, J. Dirks, P. Christensen, A combined physical and numerical simulation of tool performance in conventional deep-drawing operations, in: Proc. IDDRG 18th Biennial Congress, Lisbon, Portugal, 1994, pp. 233–240.
[21] M.P. Pereira, J.L. Duncan, W. Yan, B.F. Rolfe, Contact pressure evolution at the die radius in sheet metal stamping, J. Mater. Process. Technol. 209 (2009) 3532–3541.
[22] M.P. Pereira, W. Yan, B.F. Rolfe, Contact pressure evolution and its relation to wear in sheet metal forming, Wear 265 (2008) 1687–1699.
[23] Dassault Systèmes Simulia Corp., Abaqus Version 6. 8 Documentation, Dassault Systèmes, Providence, RI, USA, 2008.
[24] R.G. Bayer, Engineering Design for Wear, 2nd ed., Marcel Dekker, New York, 2004.
[25] W. Yan, E.P. Busso, N.P. O'Dowd, A micromechanics investigation of sliding wear in coated components, Proc. R. Soc. Lond. A 456 (2000) 2387–2407.
[26] M.B. de Rooij, D.J. Schipper, Analysis of material transfer from a soft workpiece to a hard tool: Part I—Lump Growth Model, J. Tribol. 123 (2001) 469–473.
[27] E. Schedin, B. Lehtinen, Galling mechanisms in lubricated systems: a study of sheet metal forming, Wear 170 (1993) 119–130.
[28] Z. Marciniak, J.L. Duncan, S.J. Hu, Mechanics of Sheet Metal Forming, second ed., Butterworth-Heinemann, Oxford, 2002.
[29] M. Liljengren, K. Kjellsson, T. Johansson, N. Asnafi, Die materials, hardening methods and surface coatings for forming of high extra high and ultra high strength steel sheets (HSS/EHSS/UHSS), in: Proc. IDDRG 2006 Conference, Porto, Portugal, 2006, pp. 597–604.